fortune Journals

Research Article

JOURNAL OF NANOTECHNOLOGY RESEARCH

ISSN: 2688-8521

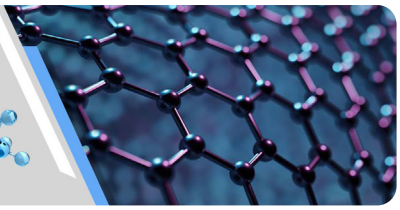

Discussion on Measurement Uncertainty Evaluation: Applied to SEM with Liquid Cell for Particle Size Measurement of Liquid Nanoparticles

Chun L Chiang[1,2*]

Abstract

In recent years, the measurement of nanomaterials or nanoparticles in liquid environments using membrane-based liquid devices coupled with scanning electron microscopy (SEM) has become an important research method for real-time and dynamic measurement. However, when measuring the mean size of nanoparticles in a liquid environment, it is a random sampling measurement, and the influencing factor model of the measurement is arbitrarily complex, making it difficult to assess the statistical dispersion. This study attempts to evaluate the measurement uncertainty of the measured values according to the requirements of JCGM 100:2008. The results show that measurement errors caused by SEM system resolution are the main source of systematic measurement uncertainty. The reproducibility of measurements of different membrane-based liquid devices is the main source of random measurement uncertainty during the measurement process. Through statistical methods, it is possible to effectively reduce the measurement uncertainty of the actual nanoparticle distribution and mean nanoparticle size within a membrane-based liquid device.

Keywords: Scanning Electron Microscopy (SEM); Membrane-Based Liquid Device; Measurement Uncertainty; Bootstrap Method; Visualization Experimental

Introduction

The application and impact of nanoparticles in liquids have gradually gained attention. Various issues such as the application of nanofluids, the efficiency of interface surfactants, and evaluation the pollution of plastic nanoparticles in water are all related to the size and concentration of nanoparticles present in the liquid [1, 2]. Using membrane-based liquid devices coupled with scanning electron microscopy (SEM) for measuring nanomaterials or nanoparticles in liquid environments has become an important research method for real-time and dynamic measurement [3]. The measurement process involves the electron beam passing through the membrane before encountering the nanoparticles within the liquid environment. Following elastic or inelastic collisions between the electron beam and the nanoparticles, the resulting backscattered electrons (BSE) and secondary electrons (SE) must also pass through the liquid and membrane before being detected by the detector [4]. Moreover, nanoparticles in liquid environments exhibit dynamic behavior due to interparticle van der Waals forces, electrical double layer forces [5], hydration forces, and Brownian motion [6], causing them to be in constant motion [7, 8]. Therefore, measuring the mean size of nanoparticles in liquid environment is a stochastic measurement, and the influencing factor model of the measurement is

Affiliation:

[1]Flow and Green Energy Research Laboratory, Center for Measurement Standards, Industrial Technology Research Institute, No. 30 Ta Hsueh Rd., Hsinchu, 30065, Taiwan

[2]Institute of Nanoengineering and Microsystems, National Tsing Hua University, Hsinchu, 30065, Taiwan

***Corresponding author:**
Chun L Chiang, Institute of Nanoengineering and Microsystems, National Tsing Hua University, Hsinchu, 30065, Taiwan.

Citation: Chun L Chiang. Discussion on Measurement Uncertainty Evaluation: Applied to SEM with Liquid Cell for Particle Size Measurement of Liquid Nanoparticles. Journal of Nanotechnology Research. 6 (2024): 27-34.

Received: May 08, 2024
Accepted: May 16, 2024
Published: June 28, 2024

Chun L Chiang., J Nanotechnol Res 2024
DOI:10.26502/jnr.2688-85210043

arbitrarily complex, making it difficult to assess the statistical dispersion [9-11]. Measurement uncertainty is a parameter associated with measurement results, used to reasonably represent the statistical dispersion of measurement results. According to JCGM 100:2008 [12], to evaluate the measurement uncertainty of measurement results, it is necessary to first establish a mathematical model representing the measurement procedure. Then, each influencing factor must be decomposed to identify all sources of error and then estimate the quantitative errors of each influencing factor. Furthermore, it is essential to evaluate the covariance of each estimation value and its sensitivity coefficient. Subsequently, the error sources of all influencing factors are combined to calculate the combined standard uncertainty and effective degrees of freedom. Then, the expanded uncertainty within the confidence interval range can be obtained. Since the error sources of various influencing factors have interactive effects, and the contributions to the measurement uncertainty are not the same in magnitude, providing partial derivatives of the mathematical model may sometimes be difficult or inconvenient due to the need for uncertainty propagation law. Additionally, the model is arbitrarily complex, and the density function of the measurement results may not be a typical continuous probability distribution, such as normal distribution or rectangular distribution; it may also be a discrete random variable, such as Poisson distribution. Therefore, according to JCGM 101:2008 [13], this type of measurement uncertainty can also be evaluated using the Monte Carlo method (MCM). Through random sampling, the probability of the appearance of random measurement values can be estimated, solving the statistical dispersion of measurement results. The bootstrapping method used in this study is a statistical method derived from the principles of MCM [14]. It involves randomly resampling from a finite sample rather than generating sampling samples randomly, to simulate the true distribution of variables.

Method

Membrane-based liquid devices are manufactured using precision processes and consist of micro reaction chambers capable of holding liquid samples. They feature a thin layer that allows for the penetration of electron beams and can be made of materials such as silicon nitride or graphene [15]. In our research, we utilized a k-kit manufactured by Bio Ma-TEK, which includes a rectangular 30 mm thickness silicon nitride membrane window measuring 300 µm in length and 25 µm in width, with a depth of 0.2 µm or 2 µm for the micro reaction chamber. The electron beam passes through the thin layer and interacts with the surface of nanoparticles within the liquid environment, resulting in both elastic and inelastic scattering. The fabrication of membrane-based liquid devices follows the sample fabrication manual provided by Bio Ma-TEK company. The liquid samples, containing nanoparticles, are filled into the channels of the membrane-based liquid devices through capillary action. Typically, the sample filling time is controlled to be within 1 minute. Subsequently, the openings at both ends of the channel are sealed with epoxy resin, and the silicon chip is placed in a vacuum chamber (1 Torr) for at least 10 minutes to ensure no leakage occurs. Finally, the sealed membrane-based liquid devices are mounted at the center of the mesh holes on a copper grid.

In this study, demonstrations were conducted using 60 nm and 30 nm gold nanoparticles from BBI Solution company. The manufacturer claims an average nanoparticle size of 59.4 nm with a normal distribution size range of 57.0 nm to 63.0 nm, and 30.1 nm with a normal distribution size range of 28.0 nm to 32.0 nm. The experiments were conducted using a Hitachi scanning electron microscope, model SU8200. The acceleration voltage was set to either 30 kV or 15 kV. The measurement process began by focusing the electron beam onto the surface of the entry thin layer of the membrane-based liquid devices. In repeated experiments, 15 random positions were selected on each membrane-based liquid device for measurement to assess repeatability. Reproducibility tests were conducted using three different membrane-based liquid devices to compare differences in the measured data. Image data analysis was performed using "Image J 1.52a" software. Default automatic thresholding methods were used to smooth and process the images by adjusting grayscale thresholds. Grayscale limits were set within the range of 0 to 130±5. Limits for nanoparticle size and circularity were set within the ranges of 0 to infinity and 0.2 to 1.0, respectively. The longest distance between two points of the nanoparticles was used to analyze nanoparticle size. The raw data were statistical analyzed using Python and Microsoft excel. The measurement data from different membrane-based liquid devices were subjected to comparison between Poisson and normal distributions, bootstrap sampling analysis to simulation the real nanoparticles size distribution in membrane-based liquid devices, we also calculation of sample means, mean standard deviation, standard error, density functions, and using ANOVA analysis to compare the measurement differences among three membrane-based liquid devices. Subsequently, an analysis of measurement uncertainty was conducted.

Results

SEM measurement involves scanning the test area from left to right and from top to bottom using an electron beam to generate raster graphic images. Each raster graphic image consists of pixels, with a one-to-one correspondence between each pixel and the pixels that generate the image on the display.

The imaging resolution affects the number of pixels per line and the number of lines in the scanning area. The effective diameter and intensity (current) of the electron beam directly affect the area where the electron beam interacts with the sample in each pixel. The effective signal comes from

Chun L Chiang., J Nanotechnol Res 2024
DOI:10.26502/jnr.2688-85210043

this interaction area, processing the signal intensity (current) from each pixel on the sample. The signal is collected and processed by the detector, which is converted into grayscale values corresponding to the display pixels. Therefore, SEM cannot distinguish samples smaller than the effective diameter, and the minimum resolution of SEM is essentially determined by the effective diameter of the spots formed by the electron beam on the sample surface. A report by Niels de Jonge and F. M. Ross in 2011 [16] indicates that the effective diameter of the electron beam penetrating the membrane after passing through is influenced by membrane thickness, density, atomic number, mass number, and accelerating voltage. The derived formula is shown in equation 1, where T represents membrane thickness, Z denotes the atomic number of the membrane material, E is the accelerating voltage of the electron beam, ρ signifies the density of the membrane material, and W represents the mass number of the membrane material.

$$d_{eff} \cong 625 \times T^{\frac{3}{2}} \times \frac{Z}{E} \times \left(\frac{\rho}{W}\right)^{\frac{1}{2}} \quad (1)$$

SEM is employed to observe nanoparticles within the membrane-based liquid devices by detecting secondary electrons. Differences between dry and liquid environments are notable. In dry conditions, as depicted in Figure 1, particles exhibit a 3D morphology. The experiment utilizes an electron beam generated by a 30 kV accelerating voltage, with a silicon nitride membrane thickness of 30 nm, and 60 nm gold particles. The image displays two discernible particles with an approximate spacing of 1.3 nm. In contrast, nanoparticle morphology in liquid environments presents a 2D appearance, as shown in Figure 2, representing images acquired by detecting secondary electrons (Figure 2a) and backscattered electrons, respectively (Figure 2b), with a halo around the particle's periphery.

Experimental results from Figure 1 and Figure 2 demonstrate significant differences in measurement outcomes between dry and liquid environments, indicating that the effective diameter of the electron beam is notably larger in liquid samples. This suggests that the being of liquid affects the effective diameter of the electron beam. Typically, SE imaging from the surface involves elastic collisions of the electron beam with electrons on the particle surface, resulting in emitted electrons providing information about surface topography. However, as demonstrated, when SEM measures nanoparticles in liquid environments, the images appear 2D, contrasting with the 3D images obtained in dry conditions. This discrepancy arises because SE are generated through elastic collisions, representing lower-energy electrons. They undergo more energy loss when penetrating through the liquid and silicon nitride membrane to reach the detector, leading to an inability to clearly depict surface morphology. A comparison of grayscale values in images from Figures 3 further supports this, showing significantly higher grayscale

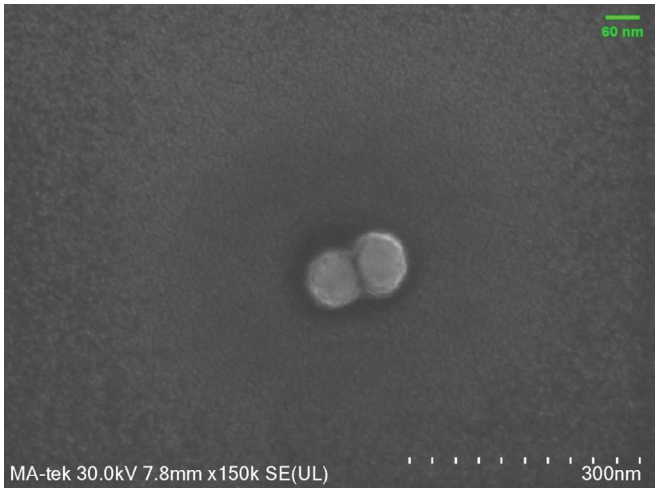

Figure 1: Using SEM to measure dried samples, primarily employing secondary electron imaging, can clearly reveal the 3D surface morphology. The particles measured are 60 nm gold particles.

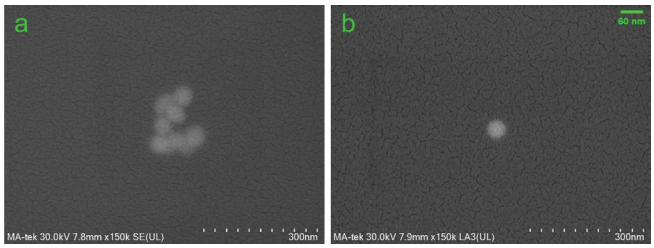

Figure 2: Comparing the differences in results obtained from SEM measurements of nanoparticles in liquid environments, the images present in a 2D format, unable to clearly display surface morphology. BSE imaging is relatively clearer than SE imaging. a is showing the SE image and b is showing the BSE image. The experiment employs a 30 kV acceleration voltage. 60 nm gold nanoparticles.

values in BSE images compared to SE images. BSE result from elastic collisions between the electron beam and atoms in deeper regions of the nanoparticles, where electrons gain energy before rebounding from the surface. Their higher kinetic energy enables them to penetrate the liquid and silicon nitride membrane more easily, explaining the higher grayscale values in their images compared to SE images. Consequently, subsequent experiments will primarily focus on analyzing images collected from BSE.

Since the evaluation of the effective radius measured by SEM also involves the accelerating voltage of the electron beam, we conducted experiments using a liquid device k-kit with a silicon nitride membrane thickness of 30 nm, a window size of 300 μm × 25 μm, and a micro reaction chamber depth of 0.2 μm. The experiments utilized a standard liquid containing 60 nm standard gold particles. Image analysis was performed using electron beam accelerating voltages of 30 kV, 15 kV, and 10 kV, with measurement results shown in Figure 4. Under different accelerating voltage operations,

Chun L Chiang., J Nanotechnol Res 2024
DOI:10.26502/jnr.2688-85210043

the grayscale values in the measurement images showed no significant differences. The particle size analysis also exhibited consistency, indicating that within the typical SEM measurement range of 30 kV to 10 kV accelerating voltage settings, there were no significant differences in the measurement results, suggesting insignificant effects on the effective diameter. Furthermore, we observed that when SEM was used for measurements and the electron beam irradiated the membrane multiple times, interactions occurred between the silicon nitride membrane and the electron beam, leading to varying degrees of carbon deposition in the affected areas. Additionally, due to the influence of the sample surface flatness, the contrast of the images may result in the so-called "edge effect" [17], where certain areas appear particularly bright. This phenomenon is more likely to occur at higher accelerating voltages.

Based on the above experimental results, we continued to use an electron beam generated by a 15 kV accelerating voltage. The membrane-based liquid devices utilized silicon nitride membranes with a thickness of 30 nm and a micro reaction chamber depth of 2 μm. The experiments focused on 30 nm gold particles, primarily collecting BSE with a detector for repeatability tests. Three sample carriers were used for reproduce experiments, with 15 non- repetitive positions selected for repeat measurement within each sample carrier window. The effective particle sizes extracted from the three experiments were 55, 66, and 57, respectively. The calculated mean particle sizes for each measurement were 30.4 nm ± 6.6 nm, 34.1 nm ±4.4 nm, and 33.7 nm ± 3.9 nm, with standard errors of 0.89 nm, 0.54 nm, and 0.52 nm, respectively. Assuming the measured values follow a discontinuous distribution, estimates were made using the Poisson distribution. The mean values were calculated to be 30.4 nm, 34.1 nm, and 33.7 nm, respectively. The results indicate an approximation to the normal distribution assumption. The cumulative distribution function plot, along with ANOVA analysis on the three sets of data, corroborates each other, with a P-value of 0.000013 indicating significant differences among the data sets. The results are presented in Table 1 and Figure 5. For detailed information, please refer to Appendix 1.

As shown in Table 2, the results of bootstrap sampling for the original data indicate that bootstrap sampling can effectively reduce the intra-group differences, leading to a more centralized trend within each group's distribution. However, bootstrap sampling and the original data are highly positively correlated, thus unable to reduce inter-group differences. Therefore, in the evaluation of measurement uncertainty, the maximum inter-group difference will be used as the basis for reproducibility assessment, while the maximum intra-group difference after bootstrap will serve as the basis for repeatability assessment. For detailed information, please refer to Appendix 2.

The measurement error caused by the resolution of the SEM system itself can be simulated using the CASINO software for Monte Carlo Simulation (CASINO stands for Monte CArlo SImulation of electroN trajectory in sOlid, taking the abbreviation from its letters, For detailed calculation flowchart, please refer to Appendix 3) [18]. Through this software, trajectories of a large number of electron beams generated in solid materials of different compositions and thicknesses can be effectively simulated. Consequently, the effective electron beam diameter (d_{eff}) at different depths can be calculated when the silicon nitride membrane thickness is 30 nm and the electron beam energy ranges from 30 keV to 15 keV. This information is then compared with experimental image interpretation to obtain the measurement error caused by the resolution of the system itself. The simulation results indicate that the effective electron beam diameter penetrating below the membrane ranges from 1.8 nm to 3.7 nm. At a depth of 100 nm below the membrane, there is no significant change in the effective diameter at 30 keV, but at 15 keV, the effective diameter increases to 16.3 nm. Therefore, the resolution of this study will be based on 16.3 nm for subsequent evaluations.

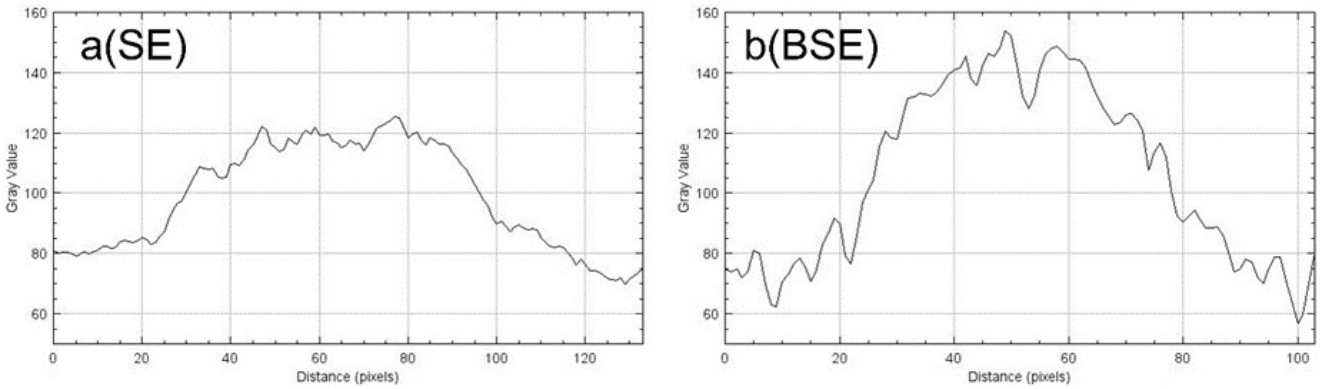

Figure 3: showing significantly higher grayscale values in b(BSE) images compared to a (SE) images. The difference in grayscale values between b(BSE) images and a(SE) images is approximately 30. This demonstrates that BSE has higher energy and is more easily detected, thus enabling imaging.

Chun L Chiang., J Nanotechnol Res 2024
DOI:10.26502/jnr.2688-85210043

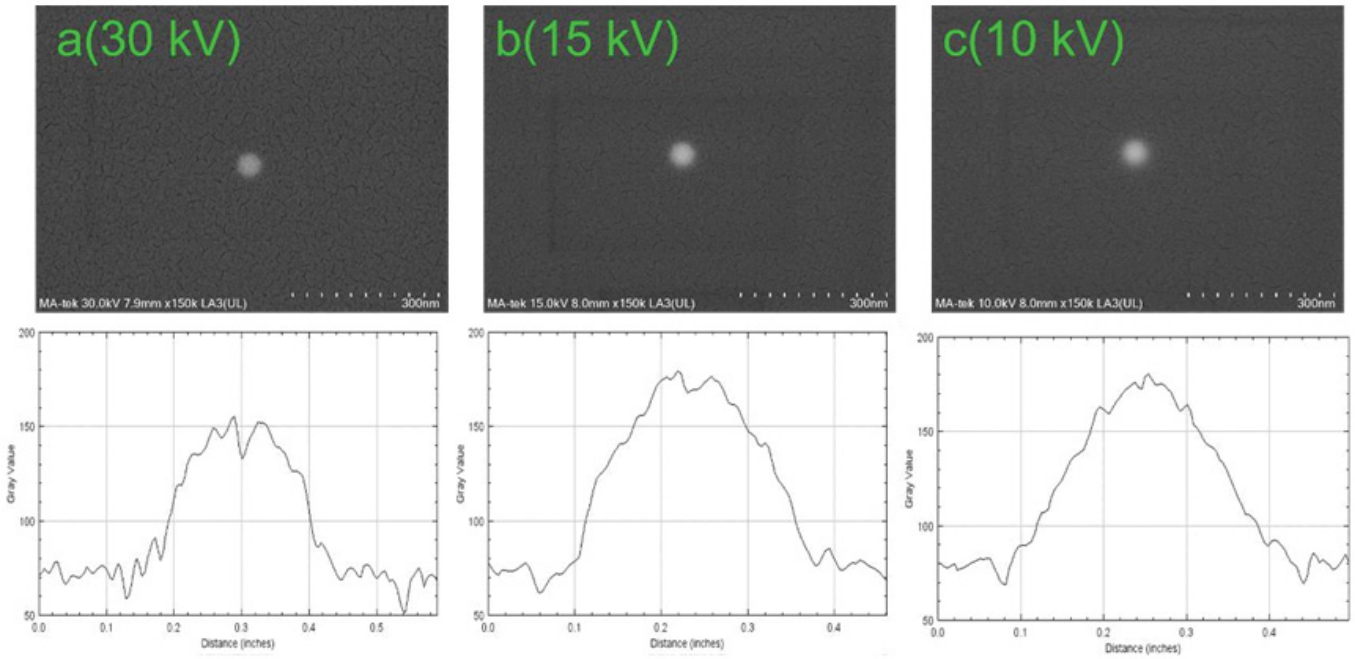

Figure 4: comparing different acceleration voltages, a(30 kV), b(15 kV), and c(10 kV), in terms of the imaging quality of the measurement results, where the measurement detects BSE imaging. The results indicate that the acceleration voltage no significant affects the grayscale values. From 30 kV to 10 kV with the grayscale value at nanoparticle being approximately 100 to 120 higher than that at background value.

Table 1: ANOVA Analysis on the Three Sets of Reproduce Experiments, Corroborates Each Other, with a P-value of 0.000013 Indicating Significant Differences Among the Data Sets.

	Degree of freedom	Sum_sq	Mean_sq	F	P
Group	2	2554.27	1277.14	11.927108	0.000013
Residual	195	20880.29	101.08	NaN	NaN

The measurement uncertainty is evaluated based on equations 2 and 3, where $\bar{x}$ represents the average particle diameter measurement, $\mu_{\bar{x}}$ represents the measurement uncertainty of the average measurement value, u_{system} represents the measurement uncertainty of the particle resolution caused by factors such as resolution and aberration of the measurement system, $u_{\text{reproducibility}}$ represents the measurement uncertainty caused by the reproducibility of particle distribution in repeated tests with different carriers, resulting in the maximum variation in particle diameter, $u_{\text{repeatability}}$ represents the measurement uncertainty of the calculated particle diameter caused by the distribution of particles within a single carrier, x_i represents each particle diameter measurement value, and n is the number of particles measured.

$$\bar{x} \pm \mu_{\bar{x}} =: \bar{x} \pm f(u_{system}, u_{reproducibility}, u_{repeatability}) = \frac{1}{n}\sum_{i=1}^{n} x_i \pm \frac{1}{2n}\sum_{i=1}^{n}[x_i - \bar{x}]^2 \quad (2)$$

$$u_{\bar{x}} = \frac{1}{2}\sum_{i=1}^{n}\{[c_{system_i}^2 u_{system_i}^2] + [c_{reproducibility_i}^2 u_{reproducibility_i}^2] + [c_{repeatability_i}^2 u_{repeatability_i}^2]\} + \left\{\frac{1}{3}\sum_{i=1}^{n}\sum_{i=1}^{n}\sum_{i=1}^{n} c_{system_i} c_{reproducibility_i} c_{repeatability_i}[u_{system} u_{reproducibility} u_{repeatability}]r\right\} \quad (3)$$

From the above explanation, the influence of each factor on measurement uncertainty may vary, and there may be interactions among the influencing factors. In this study, to estimate the minimum possible measurement uncertainty, the sensitivity coefficients of each influencing factor are initially set to +1. It is also assumed that the influencing factors are independent and unrelated to each other, with a correlation coefficient r set to 0. The measurement uncertainty contributed by the instrument mainly arises from system resolution errors. This uncertainty assessment can be conducted with reference and simulation results to existing literature for inference. For our study, with a membrane thickness of 30 nm and an accelerating voltage of 15 kV, measuring 30 nm particles in a liquid environment below the membrane at a depth of 100 nm yields an effective resolution of 16.3 nm, following a rectangular distribution. The contribution to measurement uncertainty in this case is 4.7 nm, with infinite degrees of freedom. The maximum difference in inter-group measurement values is assessed using measurement results evaluation. This occurs when situations such as 30.4 nm - 6.6 nm and 34.1 nm + 4.4 nm are encountered, resulting in a maximum difference of 14.7 nm, following a normal distribution. The contribution to measurement uncertainty in this case is 4.9 nm, with 2 degrees of freedom. For intra-group differences, the estimation is based on the average standard deviation of the mean after bootstrap for each experiment, which is 2 nm. Therefore, the contribution to measurement uncertainty is 0.67 nm, following a normal distribution. Each bootstrap is conducted 1000 times, resulting in 999 degrees

Chun L Chiang., J Nanotechnol Res 2024
DOI:10.26502/jnr.2688-85210043

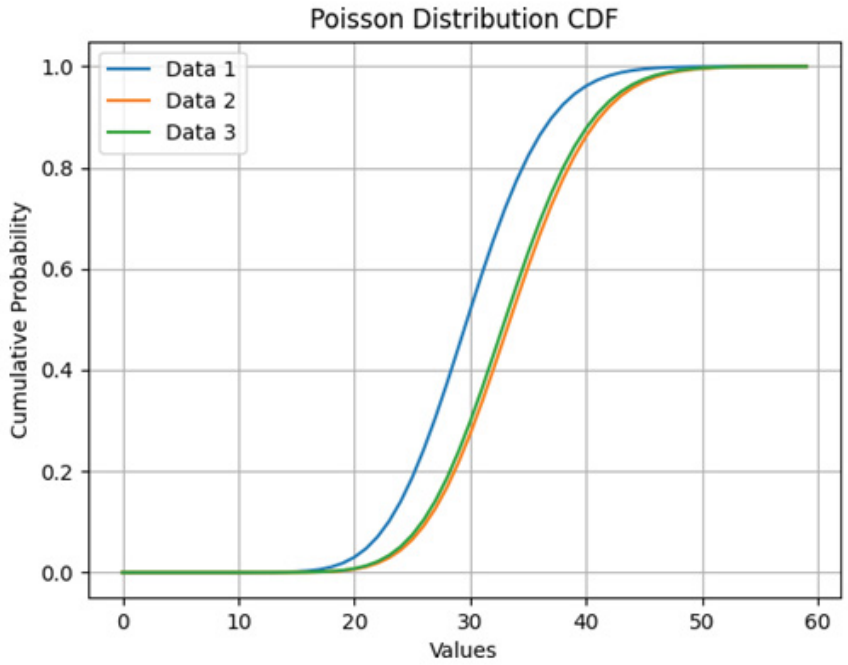

Figure 5: The cumulative distribution plot of three reproduce experiments shows that even using the same instrument, procedure, batch of particle, and membrane-based liquid devices, there may still be measurement differences due to the entire experimental process. Therefore, it is necessary to evaluate the measurement uncertainty of the entire measurement process to illustrate the data's dispersion.

Table 2: The Results of Bootstrap Sampling for the Original Data Indicate that Bootstrap Sampling from 3 Test Original Data.

Experiment 1	Count	Mean Size (nm)	S.D.	S.E.	Distribution Range	q25	q75
Measurement Data	55	30.4	6.6	0.89	(41.3, 21.1)	27.2	34.9
Python Bootstrap 1	1000	30.4	2.3	0.07	(37.9, 23.9)	28.9	32
Python Bootstrap 2	1000	30.6	2.2	0.07	(38.2, 24.2)	29	32.1
Python Bootstrap 3	1000	30.4	2.3	0.07	(36.9, 22.7)	28.9	32
Experiment 2	Count	Mean Size (nm)	S.D.	S.E.	Distribution Range	q25	q75
Measurement Data	66	34.1	4.4	0.54	(41.1, 23.1)	31	37.3
Python Bootstrap 1	1000	34.2	1.9	0.06	(39.2, 27.3)	32.9	35.5
Python Bootstrap 2	1000	34.2	2	0.06	(40.0, 28.1)	32.9	35.7
Python Bootstrap 3	1000	34	1.9	0.06	(39.3, 27.5)	32.7	35.3
Experiment 3	Count	Mean Size (nm)	S.D.	S.E.	Distribution Range	q25	q75
Measurement Data	57	33.7	3.9	0.52	(41.7, 23.2)	32	36.5
Python Bootstrap 1	1000	33.6	1.8	0.06	(38.1, 27.3)	32.4	34.8
Python Bootstrap 2	1000	33.8	1.7	0.05	(38.8, 27.8)	32.7	35
Python Bootstrap 3	1000	33.7	1.8	0.06	(40.3, 27.8)	32.5	34.9

of freedom. Thus, when each influencing factor is assumed to be independent and unrelated, the calculated value of the combined standard measurement uncertainty is 6.8 nm, with an effective degree of freedom of 7.5. At a 95 % confidence level, the coverage factor is 2.3, and the expanded uncertainty can be expressed as 15.7 nm.

Discussion

This study utilizes SEM in conjunction with membrane-based liquid devices to visualize and measure nanoparticles in liquid environments, which is the most intuitive measurement method. However, it differs significantly from traditional SEM measurements of dry samples. The electron beam reacts with the silicon nitride membrane and liquid medium during penetration, generating elastic and inelastic scattered electrons as noise. Additionally, the energy of the electron beam decreases, resulting in diffusion effects and decreased resolution. When nanoparticles in the liquid environment are hit by the electron beam, the elastic and inelastic scattered electrons produced also need to pass through the silicon nitride membrane and liquid medium to be displayed on the screen. During this process, they interact with the silicon nitride membrane and liquid medium electrons, reducing their energy or altering their path, thereby further decreasing the image resolution. As a result, the final image resolution cannot match that obtained when measuring dry samples. Based on the study by Besztejan et al. in 2017 [19], it was shown that when using an electron beam with low electron density for testing liquid samples, the measurement resolution may just reach around 10 nm that is very similar with our uncertainty evaluation. Andreas Verch et al.'s [20] research suggests that nanoparticles tend to distribute in the liquid near with the upper and lower membranes of membrane-based liquid devices due to the boundary layer effect. Due to the focusing position of the electron beam relative to the particle's position will be affected by the electron beam's reaction with the silicon nitride membrane and liquid medium during penetration, generating elastic and inelastic scattered electrons as noise. Therefore, our effective resolution simulation results limits around at 100μm depth is a reasonable derivation. Additionally, the energy of the electron beam decreases, resulting in diffusion effects and decreased resolution. When nanoparticles in the liquid environment are hit by the electron beam, the elastic and inelastic scattered electrons produced also need to pass through the silicon nitride membrane and liquid medium to be displayed on the screen. During this process, they interact with the silicon nitride membrane and liquid medium electrons, reducing their energy or altering their path, thereby further decreasing the image resolution. Consequently, the final image resolution cannot match that obtained when measuring dry samples.

Niels de Jonge et al.'s [21] study discussed that when the electron beam is focused on the entrance surface of a silicon membrane-based liquid devices and particles are distributed in the boundary layer near the entrance surface, the elastic scattering of the electron beam interacting with the liquid's component molecules occurs. This energy exchange leads to elastic scattering, increasing the diffusion of the electron beam, resulting in the phenomenon of external halo. Wayne Yang et al. [22] studied electron microscope measurements and found that the intensity of particle size measurement rose from 20 % to 80 % of its maximum height, indicating the presence of weaker signal edge-width. Comparing the papers published by Miao Song, Xiaoming Ma, and You-Jin Lee, [23], their morphologies include at least polyhedra, pyramids, rectangular prisms, rhombuses, triangular pyramids, and spheres, demonstrating that the morphological evolution of particle synthesis processes is not consistent. Moreover, since actual particles have a 3D structure and SEM images of nanoparticles in liquid environments are 2D images, and due to phenomena such as rotation, vibration, and displacement of particles in liquid environments, as reported by Yuzi Liu and See Wee Chee [24, 25], the 2D images presented by measurements are not fixed. Even the same 3D morphology may produce different 2D image differences, leading to errors in evaluating the particle size measurement. Therefore, in summary, the resolution of SEM, when used in conjunction with membrane-based liquid devices, is the main systematic error source in the measurement of particle size.

The results of scientific experiments need to be verified through multiple experiments for confirmation, followed by data organization through statistical methods. Due to factors such as the resolution of measurement equipment, control of the measurement process, measurement environment, and sample preparation, there will inevitably be measurement errors in the process of multiple measurements. Even when using the same batch of nanoparticles, the process of preparing and storing membrane-based liquid devices may deviate from reproducibility due to human factors. In the "Image J 1.52a " analysis software process, as mentioned earlier, the actual images have various forms, and using image analysis software may result in measurement errors in the final analysis due to the software's extraction parameters for each particle. For example, in this study, using the longest side of the 2D image of a single particle as a representative diameter may not necessarily reflect the actual diameter; it could also be caused by residue, particle overlap, or particle aggregation. Factors such as the spatial resolution of the SEM system and aberration compensation need to be considered, indicating that the sources of random errors in the entire experimental process need to be evaluated to confirm the reproducibility of the laboratory.

Since the area that a single SEM measurement can cover relative to the window of membrane-based liquid devices is extremely small, measurements need to be taken at

multiple different positions to obtain the particle distribution. Representing the results through the average of multiple repeated measurements is currently the most commonly used method. However, the representation of the average inevitably carries measurement errors. To explain the confidence in the measurement errors, measurement uncertainty can be used, and by defining a confidence level, the probability of measurement errors occurring can be suppressed beyond the range of 3 standard deviations, increasing the credibility of the results to over 95%. Experimental results show that using SEM to measure the particle size and distribution within membrane-based liquid devices to infer the condition of the original sample is a typical situation in statistics for estimating parameters with small samples, which may result in low accuracy and possible errors. Therefore, in this study, the bootstrap method, was used for resampling. The bootstrap method, first published by Bradley Efron [14], assumes that if the sample comes from a population that can be described by a normal distribution, its sampling distribution is also normal. However, if the population from which the sample comes cannot be described by a normal distribution, the bootstrap method also can be used for analysis. The bootstrap method satisfies both the law of large numbers and the central limit theorem, while also meeting the requirement that the bias of the sample mean deviation approximately follows a normal distribution. By using the bootstrap method, the accuracy of estimates can be improved, and measurement uncertainty reduced. Additionally, since the bootstrap method involves repeated sampling from existing data groups with replacement, generating many resampled samples, and estimating parameters from their statistics, it does not rely on randomness. Therefore, although new samples sampled from the original sample should possess characteristics of the population, they are also restricted by the population characteristics.

Conclusion

This study uses SEM in conjunction with membrane-based liquid devices to perform visualization-based measurements of nanoparticle sizes in liquid environments, providing a feasible approach for assessing measurement uncertainty regarding the measurement results. The results indicate that the measurement uncertainty caused by resolution is the main source of systematic measurement uncertainty. The reproducibility of different membrane-based liquid devices can be expressed as the measurement uncertainty of randomness during the measurement process. Through statistical methods, the accuracy of estimating the actual particle distribution and average particle size within membrane-based liquid devices using a small sample size can be effectively improved.

Acknowledgements

We thank Bio Ma-TEK for providing the TEM equipment for testing. We apologize for the membrane breakings during the test period, causing damage to the machine. We also thank ITRI for providing funding for this research.

Ethics Approval and Consent to Participate

This study does not involve this issue.

Consent for Publication

This study does not involve this issue.

Availability of Data and Materials

The research data in this article is available directly from the author upon request.

Funding

This work was supported by Industrial Technology Research Institute (ITRI).

Conflict of Interest

The authors declare there are no conflict of interests.

References

1. Hussein AK, Rashid FL, Rasul MK, et al. A Review of the Application of Hybrid Nanofluids in Solar Still Energy Systems and Guidelines for Future Prospects. Solar Energy 272 (2024): 112485.
2. Carpinlioglu MO, Kaplan M. A Comment on the Utility of Nanofluids: Interactive Influence of Nanoparticle Size and Amount at Varying Temperatures. Journal of Nanofluids 13 (2024): 536-541.
3. Suryanto B, Buckman JO, McCarter WJ, et al. In-Situ Dynamic WetSEM Imaging ANF Electrical Impedance Measurements on Portland Cement During Early Hydration. Materials Characterization 142 (2018): 86-100.
4. Ross FM. Liquid Cell Electron Microscopy. Cambridge: Cambridge University Press (2017).
5. Contini C, Schneemilch M, Gaisford S, et al. Nanoparticle–Membrane Interactions. Journal of Experimental Nanoscience 13 (2018): 62-81.
6. White ER, Mecklenburg M, Shevitski B, et al. Charged Nanoparticle Dynamics in Water Induced by Scanning Transmission Electron Microscopy. Langmuir 28 (2012): 3695-3698.
7. Ring EA, de Jonge N. Video-Frequency Scanning Transmission Electron Microscopy of Moving Gold Nanoparticles in Liquid. Micron 43 (2012): 1078-1084.
8. Liu Y, Lin XM, Sun Y, et al. In Situ Visualization of Self-Assembly of Charged Gold Nanoparticles. Journal of the American Chemical Society 135 (2013): 3764-3767.

9. Barisik M, Atalay S, Beskok A, et al. Size Dependent Surface Charge Properties of Silica Nanoparticles. The Journal of Physical Chemistry C 118 (2014): 1836-1842.

10. Francois L, Mostafavi M, Belloni J, et al. Optical Limitation Induced by Gold Clusters. 1. Size Effect. The Journal of Physical Chemistry B 104 (2000): 6133-6137.

11. Egerton RF, Li P, Malac M. Radiation Damage in the TEM and SEM. Micron 35 (2004): 99-409.

12. JCGM: Joint Committee for Guides in Metrology 100:2008. Evaluation of Measurement Data: Guide to the Expression of Uncertainty in Measurement. Geneva: JCGM (2008).

13. JCGM 101:2008. Evaluation of Measurement Data: Supplement 1 to the "Guide to the Expression of Uncertainty in Measurement" Propagation of Distributions Using a Monte Carlo Method. Technical Report. Geneva: JCGM (2008).

14. Efron B. Bootstrap Methods: Another Look at the Jackknife. Annals of Statistics 7 (1979): 1-26.

15. Kelly DJ, Zhou M, Clark N, et al. Nanometer Resolution Elemental Mapping in Graphene-Based TEM Liquid Cell. Nano Lettres 18 (2018): 1168- 1174.

16. De Jonge N, Ross FM. Electron Microscopy of Specimens in Liquid. Nature Nanotechnology 6 (2011): 695-704.

17. Hafner B. Scanning Electron Microscopy Primer, Characterization Facility. Minnesota: University of Minnesota-Twin Cities (2007).

18. El Azzouzi M, Khouchaf L, Achahbar A. Montecarlo Study of the Interaction Volume Change by the Beam Skirt in VP-SEM. Acta Physuca Polonica A 132 (2017): 1393-1398.

19. Besztejan S, Keskin S, Manz S, et al. Visualization of Cellular Components in a Mammalian Cell with Liq-Uid-Cell Transmission Electron Microscopy. Microscopy and Microanalysis 23 (2017): 1-10.

20. Verch A, Pfaff M, de Jonge N. Exceptionally Slow Movement of Gold Nanoparticles at a Solid/Liquid Interface Investigated by Scanning Transmission Electron Microscopy. Langmuir 31 (2015): 6956-6964.

21. de Jonge N, Houben L, Dunin-Borkowski RE, et al. Resolution and Aberration Correction in Liquid Cell Transmission Electron Microscopy. Nature Reviews Materials 4 (2019): 61-78.

22. Yang W, Zhang Y, Hilke M, et al. Dynamic Imaging of Au-Nanoparticles via Scanning Electron Microscopy in a Graphene Wet Cell. Nanotechnology 26 (2015): 315703.

23. Song M, Wu Z, Lu N, et al. Strain Relaxation-Induced Twin Interface Migration and Morphology Evolution of Silver Nanoparticles. Chemistry of Materials 31 (2019): 842-850.

24. Liu Y, Lin XM, Sun Y, et al. In Situ Visualization of Self-Assembly of Charged Gold Nanoparticles. Journal of the American Chemical Society 135 (2013): 3764-3767.

25. Chee SW, Baraissov Z, Loh ND, et al. Desorption-Mediated Motion of Nanoparticles at the Liquid–Solid Interface. The Journal of Physical Chemistry C 120 (2016): 20462-20470.